Journal of Applied Polymer Science

Human-lymphocyte cell friendly starch-hydroxyapatite biodegradable composites: Hydrophilic mechanism, mechanical, and structural impact

Sumit Pramanik[1], **Pratibha Agarwala**[1,2], **Kharthik Vasudevan**[1], **Koustav Sarkar**[3]

[1]Composite Laboratory, Department of Mechanical Engineering, SRM Institute of Science and Technology, Kattankulathur, Kancheepuram 603203, Chennai, Tamil Nadu, India

[2]Department of Medicinal Chemistry, Central University of Punjab, Punjab, India

[3]SRM Research Institute and Department of Biotechnology, SRM Institute of Science and Technology, Kattankulathur, Kancheepuram 603203, Chennai, Tamil Nadu, India

Correspondence to: S. Pramanik (E-mail: sumitprs@srmist.edu.in or prsumit@gmail.com)

ABSTRACT: Biodegradable starch (Str) polymer was derived from potato, a plant-based natural carbohydrate polymers source, by one-pot synthesis. Hydroxyapatite (HA) was produced from goat bone by step sintering. The inexpensive starch/HA thin film composites were fabricated by customized spin coating. This study revealed that the hydrogen bond energy and distance have significant effect on glass transition temperature of the polymer. The 40 wt % HA contained starch (StrHA40) composite thin film showed excellent tensile strength (3.03 + −0.03 MPa), elongation (21.5 + −5.5%) and modulus (15.5 + −0.2 MPa) closed to human skin. The *in vitro* swelling and biodegradation kinetics of pristine starch and pure HA has been controlled and improved by using suitable composition. This study postulated the probable water molecule-adsorption mechanisms of pristine starch and starch/HA composite films. The StrHA40 composite showed excellent biocompatibility to the human-blood derived lymphocyte cells. Therefore, the starch/HA thin film composite-based biodegradable scaffolds developed in the present study can be an excellent potential candidate for soft tissue regeneration and/or replacement applications. © 2019 Wiley Periodicals, Inc. J. Appl. Polym. Sci. **2020**, *137*, 48913.

KEYWORDS: biodegradable; biomedical applications; differential scanning calorimetry (DSC); glass transition; synthesis and processing techniques

Received 25 July 2019; accepted 4 December 2019

DOI: 10.1002/app.48913

INTRODUCTION

Biomedical applications of biodegradable and biocompatible polymers generate an enormous research interest to the present world.[1,2] Uses of biodegradable polymers in biomedical fields including, wound dressings, drug delivery applications, surgical implants, and other medical devices have grown profoundly due to their good biocompatibility, biodegradability and their degradation products, which are nontoxic and have proper mechanical as well as degradation kinetic properties.[3] Several synthetic thermoplastic polymers, such as poly(lactic acid) (PLA), poly (α-hydroxyl acids) (PHA), poly(glycolic acid), poly(L-lactic acid), poly(lactic-*co*-glycolic acid), and so on have been developed as biopolymers for biomedical uses.[4] However, cost of these synthetic biopolymers is very high and they are not abundant. One of the major disadvantages of these conventional biopolymers is that the local pH value decreases after their degradation. As a result, these polyesters-like conventional biopolymers accelerate degradation rate and help to induce an inflammatory reaction. Further demerit of those highly porous scaffolds biopolymers, for example, PHA, is weak in mechanical properties. In contrast, biopolymers of starch-based carbohydrate polymers showed some fascinating properties. Starch can be hydrolyzed into glucose by microorganism or enzymes, and then metabolized into carbon dioxide and water. It has a greatest potentiality among polysaccharides owing to its excellent ability to form a continuous matrix in addition to its abundant, renewable, and low cost.[5] It exists in many forms depending on the origin of raw materials.[6] Starch-based biodegradable polymers have several advantages in biomedical applications due to their good biocompatibility, biodegradability, and nontoxic degradation products, and so on.[3] However, the starch-based polymers have still unsatisfactory mechanical properties and uncontrollable degradation. Interestingly, the microsphere or hydrogel form of the starch-based polymers is ideal for drug delivery.[7] It can avoid the risk of surgical removal of the device after drug depletion.[8] Therefore, starch would be used as promising biopolymer in coming days. The

main reasons for the selection of starch-based material in the present investigation are that: (1) it is inexpensive due to its abundant sources and (2) the extremely low manufacturing cost since it is extracted from various foods such as rice, wheat, maize, potato, corn, and so on.[9] Broadly, the starch is used as a biodegradable material in three methods: (1) high-amylose starch can directly be converted into strong biodegradable plastic film; (2) small-granule starch can be used as filler in other polymers, for example, polyethylene (PE) film (6–15%) which is degraded via cleaving of polymer chains by peroxides produced in presence of antioxidants; and (3) high-starch-containing mixtures (40–60%) can be used as a destructurized form of the polymer film. Synthesis of starch processing also involves different procedures such as, heating, pregelatinizing (develops cold-water-soluble starches without heating), and chemical modification (develops crosslink formations between starch and components via functional groups owing to the produced hydrophobic starch derivatives or dialdehyde starch). However, starch has not been used successfully because of its poor mechanical properties, uncontrollable biodegradation, low dimensional stability, and less processability. In this context, ceramic materials might be useful for tuning the mechanical properties of these polymers.[1] Among the bioceramics, hydroxyapatite [HA, $Ca_5(PO_4)_3(OH)$], a form of calcium phosphate, shows best biocompatibility in physiological conditions. HA is a naturally occurring mineral similar to the morphology and composition of human hard tissues.[4] HA can be synthesized by various techniques, such as hydrothermal,[10] wet chemical,[11] sol–gel,[12] and solid-state reaction[13] from several sources such as, different synthetic compounds, including calcium oxide,[11] calcium nitrate,[12] natural coral rock,[14] cockle shell,[15] egg shell,[16] as well as bones.[17,18]

Composite materials show an excellent desired strength and toughness. The natural bone is organic collagen polymer/inorganic calcium phosphate-based composite. It is well established that HA mimics the natural bone mineral[19] and has been found to possess good mechanical, biocompatible, and osteoconductive properties in bone.[20] In another study, it was found that PE glycol impregnated HA-based composite had shown excellent biocompatibility to the human skin derived fibroblast cells.[17] The skin cells also composed of collagen-based composites with different proteins and lipids. From this point of view, composite materials are better choices as tissue engineering scaffolds. In this context, long-term intake of raw potato starch may induce a change in the colonic environment by reducing damage to colonocytes, diminishing colonic and systemic immune reactivity, and improving mucosal integrity.[21] It turns benefit to health where inflammatory conditions are associated. However, no lymphocyte cell proliferation test on potato starch-based biodegradable materials has been investigated properly till date.

To evaluate the *in vitro* biocompatibility of the materials several *in vitro* culture assays are available. Most of these systems are based on the assessment of the cell death, adhesion, proliferation, morphology, and biosynthetic activity.[22–24] The biodegradable composite scaffolds might be used for different biological applications, including, repair or regeneration of bone, skin, and membranes.

Therefore, this present work first aimed to use the simple extraction methods of the starch from potato and the HA bioceramic from goat bones. Since no thin film scaffold of biodegradable starch-/HA-based composites has been reported so far, this present study for the first time, aimed to fabricate the starch/HA thin film composites-based biodegradable scaffolds derived from natural sources in order to make them cheap compared to the other synthetic biopolymer-based materials. This work mainly focused to predict an optimal amount of starch–HA composites that would be used as a potential candidate for biodegradable scaffold in tissue engineering applications. The chemical structure and bonding of starch polymer and its composites have been analyzed precisely by X-ray diffraction (XRD), calorimetric, and spectroscopic analyses. This study also exclusively determined the water adsorption mechanisms of the composite in order to explore the role of the hydrogen bonds in carbohydrate polymers and the ceramics particles on mechanical properties, biodegradability, and hydrophilicity. Since the present material has several biomedical engineering applications, the cell proliferation and viability of the synthetic starch-based composites had, for the first time, been evaluated on the human blood derived lymphocyte cells.

EXPERIMENTAL

Materials and Methods

Extraction of Potato Starch. The main ingredients used for the extraction of starch are potatoes (*Solanum tuberosum*) and distilled water. The starch content in the vegetables varies depending upon the plant source. Since potato contents huge amount of starch compared to the other plants or vegetables, it was selected as best source of starch production. A measured amount of raw potatoes were taken and cleaned several times under running water.[25] The outer skin of the potatoes was peeled out. The peeled potatoes were ground in a blender and then, distilled water was added at a ratio of 1.5:1 (w/v) to the slurry and stirred vigorously. The slurry was then filtered followed by kept for 3 h to obtain starch. The wet starch was dried at normal atmospheric conditions to obtain a white in color starch powder.

Preparation of HA Bioceramic Powder. The HA used as a bioceramic filler powder was produced from goat bone (i.e., vertebrate animal as natural sources) by step sintering technique reported by other study.[26] Here, raw ingredient used for the synthesis of HA is goat bones. Goat bones of age around 2 years were purchased from local store. The muscles and ligaments were thoroughly cleaned out being boiled in distilled water for 30–45 min. After boiling, the bones were dried for few days at normal atmospheric conditions. The dried bones were then sintered at 500 °C for 2 h followed by 900 °C for 4 h. The furnace cooled sintered bones were then ground into white in color fine ceramic powder, which would be used to prepare the composite biomaterials.

Preparation of Thin Film Using Potato Starch and its Composite. Biodegradable starch (Str) polymer was synthesized by one-pot synthesis technique. The starch extracted from potato, which is a cheapest plant-based natural source. The synthesized potato starch powder was first dissolved in distilled water at around 0.28 (w/v) ratio.[27] The glycerol (Technical grade, M/s Srihari Scientific) was then added to the starch solution at a ratio of 1.4 (w/v)

glycerol:starch while acetic acid (Commercial grade, M/s Srihari Scientific) was used at a ratio of 0.7 (w/v) acetic acid:starch. The mixture was then stirred vigorously at 120 °C for 15–20 min using a magnetic hot plate to get a thick paste. The produced dense gum-like paste was then transferred onto a moving glass Petri dish and held for spinning at around 1300 rpm to get a thin film using customized spin-coating technique. The entire synthesis reaction of starch polymer from potato starch powder (polysaccharide) is depicted in Scheme 1. Here, glycerol was used as a plasticizer and also it would make the bioplastic more flexible while acetic acid would enhance the ionization of the polymerization reaction resulting to get more homogenous biopolymer film.

In case of composite, the synthesized HA powder was mixed with the starch polymer being heated with various compositions of apatite, such as 10, 40, 60, and 90 wt %. Then, the composite thin film of thickness 200–300 μm scaffolds were produced similar to the process of pristine starch film formation. The freshly produced composite films were analyzed by different suitable characterization techniques. The whole synthesis method is depicted schematically in Scheme 1. The sample codes and their description used for this study are illustrated in Table I.

Table I. Sample Code and Description Used in this Study

Sample code	Description
HA	Bone was sintered at first 500 °C for 2 h and then 900 °C for 4 h and then was ground into powder as pure HA
Str	Pristine starch
StrHA10	Composite of Starch and 10 wt % HA
StrHA40	Composite of Starch and 40 wt % HA
StrHA60	Composite of Starch and 60 wt % HA
StrHA90	Composite of Starch and 90 wt % HA

Characterizations

Microstructure. Microstructure of the composite specimens was viewed by light optical metallurgical microscope (BX-KMA-LED, Olympus, Japan). Field emission scanning electron microscope (QUANTA 200; FEI) was also used to explore additional supportive information on the microstructure of all the specimens.

Density. Bulk density (ρ in g cc^{-1}) of the composites samples was conducted by modified Archimedes' principle using eq. (1) employing a weighing balance of resolution ±0.0005 g as reported elsewhere.[18,28] The measurement was conducted using in-house weighing method to take the weight of the immerged samples at suspended condition using the simple weighing balance only. At least three identical specimens were used to calculate the mean density of both the samples.

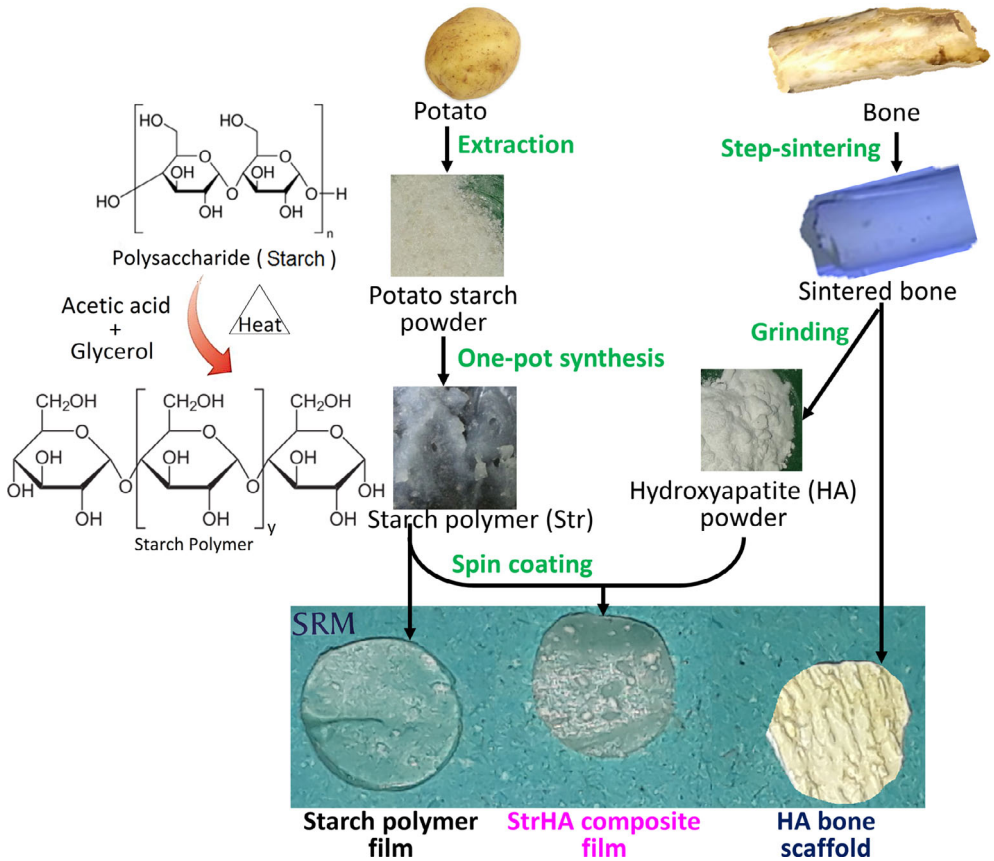

Scheme 1. Schematic representation of synthesis and fabrication of starch, HA, and their composite films. [Color figure can be viewed at wileyonlinelibrary.com]

$$\rho = \frac{M_{air}}{M_{immeresed}} \times \rho_{water} \quad (1)$$

where M_{air} is the mass (g) in air, $M_{immersed}$ is the mass (g) in water during fully immersed specially suspended condition which is equivalent to the bulk volume of sample, and ρ_{water} is the specific gravity of water at room temperature (25 °C).

Tensile. Mechanical properties of the composite specimens were determined by tensile strength and elongation using universal tensile machine [TUE-CN-400, FSA (P) Ltd., India] at a cross-head speed of 1 mm min^{-1}. The rectangular triplicate specimens of cross section of 3–6 mm^2 and length of 12–18 mm were used for the tensile test.

X-ray Diffraction. XRD study of the composite films as well as pristine starch film and pure HA powder was conducted in the range of diffraction angle, 2θ = 10–50° of Cu Kα radiation using X-ray diffractometer (X'Pert Pro; PANalytical, UK) at normal scanning.

Fourier Transform Infrared Spectroscopy. Fourier transform infrared (FTIR) spectroscopy of the selected composite film as well as pristine starch film and pure HA powder was conducted in the range of wavenumber 4000–500 cm^{-1} using infrared spectrometer [IRTracer-100AH(EN230V), Shimadzu Corporation, Japan] at a resolution of 4 cm^{-1} of quad scan.

Differential Scanning Calorimetry. Differential scanning calorimetry (DSC) of pristine starch and StrHA40 composite of nearly 10 mg each sample sealed in an aluminum pan was performed using a DSC (214 Polyma; NETZSCH DSC, Germany) with an internal coolant, nitrogen purge gas of flow rate 10 mL min^{-1}, and scanned from −15 to 150 °C at a rate of 10 °C min^{-1}. It was done to analyze the endothermic melting (T_m) as well as glass transition (T_g) behaviors of the pristine starch and StrHA40 composite films. Since the main focus of this study was to determine the starch properties and the most important composite, the technique DSC was eliminated for other composite materials. At low temperature range, HA ceramic also does not show any significant change in DSC.

***In Vitro* Biodegradation Kinetics.** *In vitro* biodegradation study on the composite thin film scaffolds was conducted at 25 °C in saline water up to 17 days by continuing checking of their change in weight at different intervals. Each result of the materials Str, StrHA40 and HA showed first swelling or increase in weight then a degradation or decrease in weight. The normalized weight percentage (W) was calculated using eq. (2). Using the degree of swelling,[29] the first-order swelling (K_{Swell}) and degradation ($K_{Degrade}$) rate constants (min^{-1}) were calculated separately by eqs. (3) and (4), respectively.[30]

$$W = \frac{M_t}{M_i} \times 100\% \quad (2)$$

$$K_{Swell} = \frac{1}{t}\left[\frac{W_f - W_i}{W_f - W_t}\right] \quad (3)$$

$$K_{Degrade} = \frac{1}{t}\left[\frac{W_i - W_f}{W_i - W_t}\right] \quad (4)$$

where M_i is the initial weight (g) of each scaffold, M_t is the weight (g) of the scaffold at time t (min), W_i is the initial normalized weight fraction of each scaffold, and W_t is the normalized weight fraction of the scaffold at time t; and W_f is the normalized weight fraction of the scaffold at the end of swelling or degradation reaction after complete the swelling or degradation study, respectively.

***In Vitro* Cell Culture Assay.** For the first time, *in vitro* biocompatibility study of the starch–HA composites was carried out on human blood cell derived lymphocytes. To achieve the aim of this study, the blood cell derived lymphocytes response of the most important and optimized composite, that is, StrHA40 was only selected to compare with pristine starch and pure HA. The other composites were eliminated due to the lack of particular applications in biomedical engineering applications. In this *in vitro* assay first, the lymphocytes were isolated from peripheral blood mononuclear cells of human blood.[31] Lymphocytes were grown as monolayer cultures in HyClone RPMI 1640 media (GE Healthcare Life Sciences) supplemented with 10 vol % fetal bovine serum, 2 vol % penicillin streptomycin. Lymphocytes were seeded at a density of 10^6 cells/well in 24-well plates (n = 5) on the three different type samples such as fully transparent pristine starch film, partially transparent StrHA40 composite film, and opaque HA scaffolds of 6 mm diameter × 1 mm thick. The negative control was prepared with supplemented media solution containing cells but without addition of any scaffold in the 24-well plate of standard poly(methyl methacrylate)-based plastic. The whole cell culture study was carried out up to 3 days.

In parallel, lymphocytic proliferation was checked by tetrazolium salt, 3-(4,5-dimethylthiazol-2-yl)-2,5-diphenyltetrazolium bromide (MTT) assay as described earlier.[32] Lymphocytes were seeded in 96-well plates (n = 5), at a density of 2×10^5 cells/well. The cell culture was done as mentioned above for 3 days on the three different type samples such as fully transparent pure starch film, partially transparent StrHA40 composite film, and opaque HA scaffolds. In brief, 20 µL of MTT solution (5 mg m^{-1}) was added in above mentioned each of cell culture well and incubated for 4 h at 37 °C. The medium was removed by aspiration and the purple colored formazan precipitate was dissolved in 100 µL dimethyl sulfoxide and optical density (OD) or absorbance was measured at 565 nm using a microplate reader (Tecan Spectra, Grodig, Austria).[33]

RESULTS AND DISCUSSION

Microstructure

Figure 1(a–e) depicts the micrographs of the starch/HA-based composites, including pristine starch, StrHA10, StrHA40, StrHA60, and StrHA90. The intact structure of pristine starch closely resembled with other studies.[34] It also reveals that the homogeneous distribution of HA particles in the starch matrix can be done up to 40 wt % of HA particles. In addition, some interconnecting pores also appeared in the microstructure of StrHA40 composite scaffold. The presence of less than 90 µm size

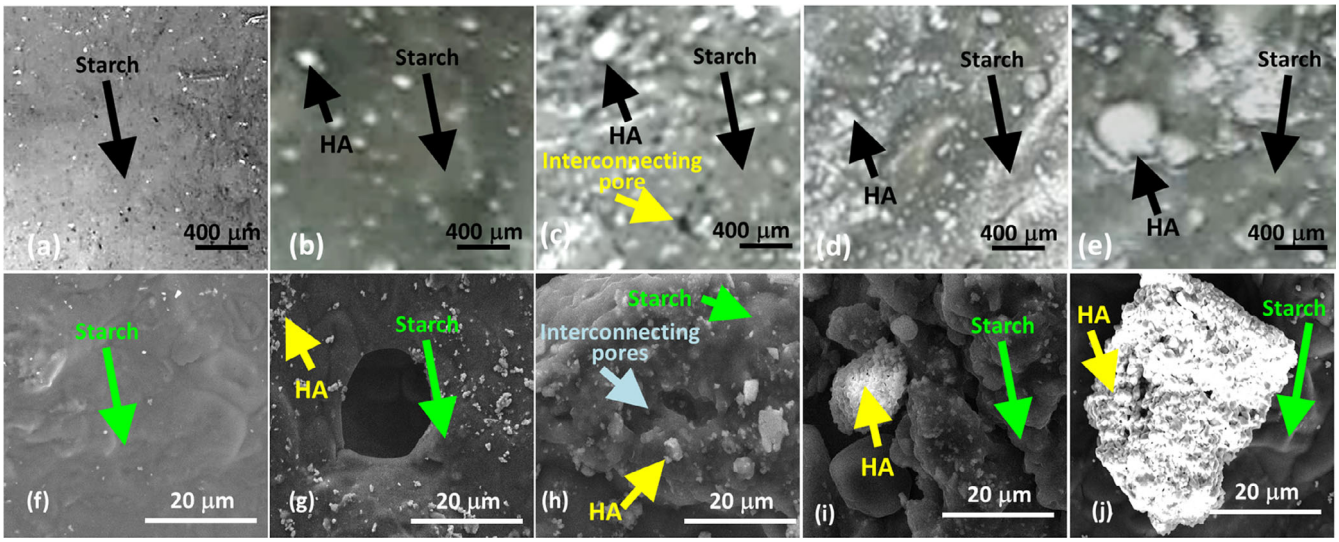

Figure 1. Optical micrographs of (a) pristine starch (Str), (b) StrHA10, (c) StrHA40, (d) StrHA60, and (e) StrHA90 films; and SEMs of (f) pristine starch (Str), (g) StrHA10, (h) StrHA40, (i) StrHA60, and (j) StrHA90 films. [Color figure can be viewed at wileyonlinelibrary.com]

particles was confirmed in the high-resolution optical micrographic images in Figure 1(b,c). Above 40 wt % HA, the HA particles was found to form agglomerates. It was observed in the StrHA60 and StrHA90 composites [see Figure 1(d,e)]. Agglomeration might be occurred due to particle size of HA in nanoscale as predicted by other report.[33,35] Also at higher HA content composites (StrHA60 and StrHA90), the interconnected type pores disappeared and even many large agglomerated particles appeared. Similar particles and pore behaviors were observed in the FESEM images from Figure 1(f–j). In FESEM study, the nanosized HA particles (up to 400 nm) were also found in the composites, particularly up to 40 wt % HA contents in Figure 1 (g,h) but after that the HA particle had agglomerated and in some cases, they came out of the starch matrix as revealed in Figure 1(i,j). Therefore, in this starch and HA system, maximum 40 wt % of HA particles in the starch matrix would be the best optimized composition compared to the other compositions.

Density

Density of the starch, HA, and their composites measured by modified Archimedes' principle is illustrated in Table II. The result indicates that their density increases with increasing of HA content linearly. The density of starch film is slightly higher than the potato starch powder (i.e., 0.763 g cc^{-1})[36] because of the polymerization.

Tensile

The tensile stress–strain behavior of all the starch/HA-based composites is depicted in Figure 2. The tensile mechanical properties of the starch/HA-based composite films are illustrated in Table II. This result reveals that tensile properties increased with HA content do not increase linearly. Initially, the ultimate tensile strength (UTS) increased up to 40 wt % of HA in starch content (i.e., StrHA40 composites) but above that strength decreased while tensile elastic modulus increased up to 10 wt % HA in starch (i.e., StrHA10 composite). The thin film scaffolds up to 40 wt % HA in StrHA40 composite film showed best tensile mechanical properties in terms of high UTS (>3 MPa), low modulus and optimum elongation (E > 21%) or toughness in our present investigation. The highest elongation was observed for pristine starch (Str) film might be due to its high cohesive energy. However, the elongation of pure apatite bioceramic was reported as less than 15%.[13] Therefore, present result might be attributed to the agglomeration formation during processing of composite above 40 wt % HA in starch which could be confirmed by microscopic analysis in Figure 1. The uniform distribution of second

Table II. Density and Tensile Properties of the Composite Films

Sample code	Density ± standard deviation (SD) (g cc^{-1})	UTS ± SD (MPa)	Young's modulus ± SD (MPa)	Elongation ± SD at UTS (%)
Str	0.82 ± 0.02	0.28 ± 0.06	5.024 ± 0.024	76.18 ± 5.5
StrHA10	1.26 ± 0.06	0.3 ± 0.035	15.078 ± 0.375	19.03 ± 8.0
StrHA40	1.31 ± 0.03	3.03 ± 0.030	15.692 ± 0.174	21.5 ± 5.5
StrHA60	1.46 ± 0.06	1.74 ± 0.055	5.977 ± 0.573	38.09 ± 9.0
StrHA90	1.71 ± 0.03	1.06 ± 0.085	5.306 ± 0.774	42.31 ± 9.5
HA	2.89 ± 0.23	—	—	—

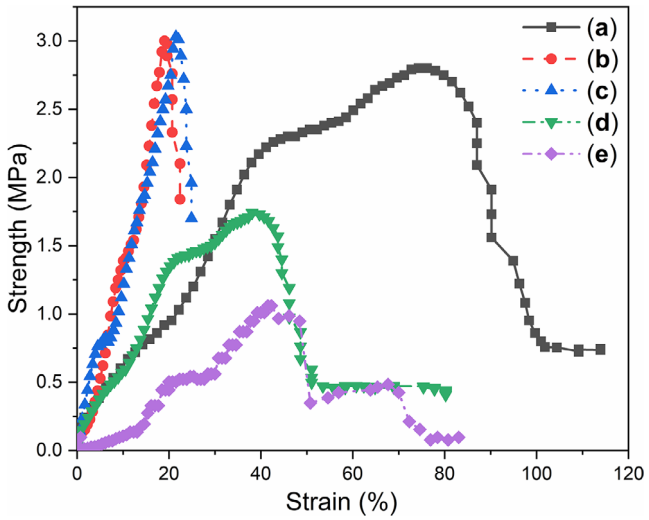

Figure 2. Tensile stress–strain relation of (a) Str, (b) StrHA10, (c) StrHA40, (d) StrHA60, and (e) StrHA90 film samples. [Color figure can be viewed at wileyonlinelibrary.com]

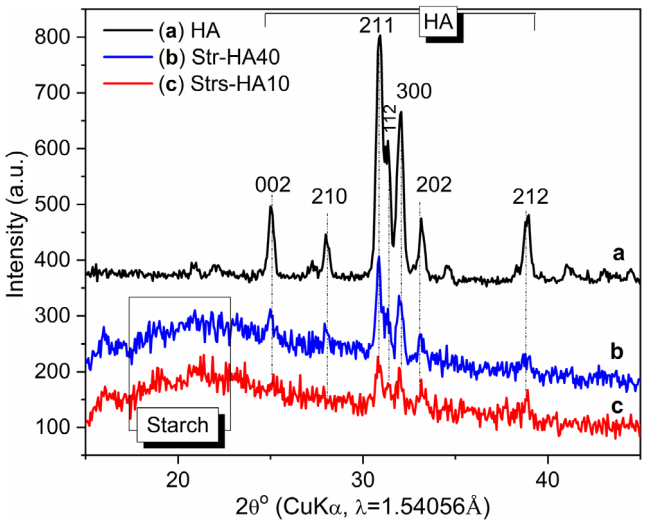

Figure 3. XRD patterns of (a) Pure HA, (b) StrHA10, and (c) StrHA40 composites. [Color figure can be viewed at wileyonlinelibrary.com]

phase HA particles was found up to 40 wt % in the starch matrix. Since the StrHA40 composite thin film had shown best tensile strength, elongation as well as modulus, this composite was selected for further structural and biological studies. It is to be informed that all the mechanical properties of all the measured samples are significantly higher compared to starch polymer reported by other studies.[37] Furthermore, the UTS (0.28 ± 0.06–3.03 ± 0.03 MPa) and moduli (5.024 ± 0.024–15.69 ± 0.17 MPa) of the present composite films were very close to the human skin (UTS ≈ 1.2–1.9 MPa in transverse direction and $E \approx 14.96$ MPa).[38]

X-ray Diffraction

XRD patterns of pure HA sintered at 900 °C/4 h, Starch-HA10 (StrHA10), and StrHA40 composites are depicted in Figure 3. The main identification XRD crystalline peaks of the sintered bone powder resembled with the XRD file of JCPDS No. 00-009-0432 of standard HA as found at 2θ of between 31 and 35°. The broad amorphous peak appeared in the range of 2θ = 12–26° attributed to starch polymer. Both amorphous as well as crystalline peaks were found in the StrHA40 composite film. It indicates that the homogeneity of the HA particles in the starch matrix is good.

Fourier Transform Infrared

The functional bonds present in the pristine starch, StrHA40 composites and pure HA have been confirmed by the FTIR spectroscopy depicted in Figure 4. The broad band represented by **1** at 3278 cm^{-1} in starch attributed to the stretching mode of O—H groups. The absorption band marked by **3** at 1647 cm^{-1} attributed to an intermolecular H-bond involving the carboxyl group.[39] The peak at 2929 cm^{-1} marked as **2** attributed to C—H stretching, the bands at 1159 cm^{-1} marked as **5** assigned to C—O, 1002 cm^{-1} marked as **6** assigned to primary O—H as well as —O— group and the 855 cm^{-1} marked as **7** is indication of for β-configuration.[40–42] The presence of a band marked as **4** at 1416 cm^{-1}, attributed to the C═H stretching vibration of CH_2.[40] The three identification peaks at 3307, 1044, and 621 cm^{-1}, marked as **8**, **9**, and **10**, respectively, were found for pure HA.[17] The broad band at 3307 cm^{-1} is due to the OH stretch vibration of HA. The peaks at 1034 and 621 cm^{-1} assigned to phosphate group of HA. In the StrHA40 composite, both the peaks of pristine starch as well as pure HA were observed. It clearly indicates that there was no formation of extra chemical bonding between the starch polymer chains and HA ceramic particles. However, since the O—H (see Peak **1**) and C—H (see Peak **2**) stretching peaks of starch part reduced significantly in the composite (StrHA40), there might be a chance of steric hindrance between the molecular —OH of HA and —CH_2—OH of starch. It would have further profound effect on swelling as well as biodegradation rate. Thus, HA molecules change the intramolecular hydrogen bond vibration in the starch which is made of similar monomer group of cellulose.

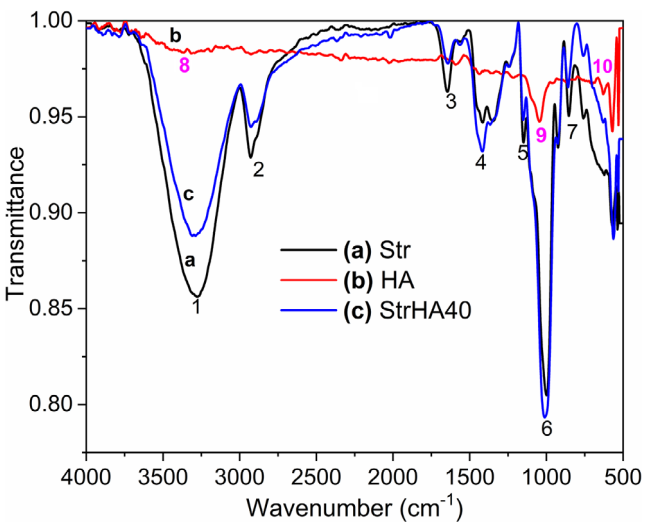

Figure 4. FTIR spectra of (a) pristine Str, (b) pure HA, and (c) StrHA40. [Color figure can be viewed at wileyonlinelibrary.com]

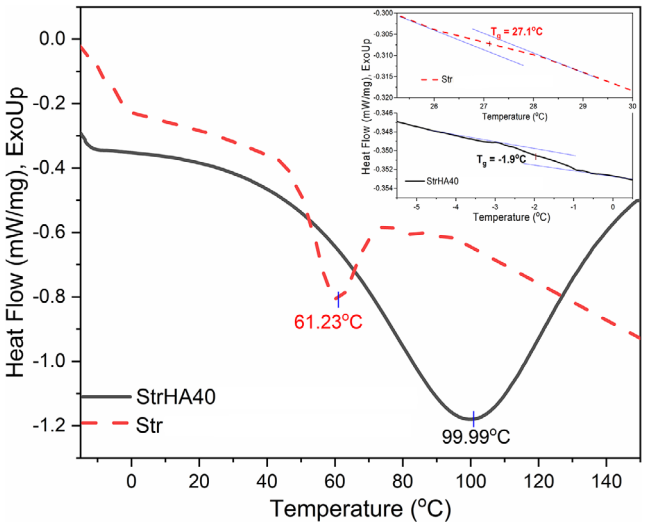

Figure 5. DSC thermograms of (a) Str (firm line) and (b) StrHA40 (dash line) composite, and Inset image represents the glass transition temperature (T_g). [Color figure can be viewed at wileyonlinelibrary.com]

The intramolecular hydrogen bond of pristine starch (3307 cm^{-1}) has shifted to 3278 cm^{-1} in the StrHA40 composite and it indicates that the formation of monoclinic I_β allomorphs of starch-repeating unit. The hydrogen bond energy (E_H) and hydrogen bond distance (R_H) of the OH stretching vibration mode of the materials were computed as 26.684 kJ and 0.2756 nm for pristine starch film and 24.629 kJ and 0.2763 nm for StrHA40 composite film, using eqs. (5) and (6).[43,44]

$$E_H = \frac{1}{k}\left[\frac{\Delta\nu}{\nu_{std}}\right] \quad (5)$$

$$R_H = c - \frac{\Delta\nu}{b} \quad (6)$$

where $\Delta\nu = \nu_{std} - \nu$, ν_{std} is the standard frequency corresponding to free OH groups (3650 cm^{-1}), ν is the frequency of the bonded OH groups of the specimens, and the constants $k^{-1} = 2.625 \times 10^2$ kJ, $b = 4430$, and $c = 2.84$. The lesser E_H and longer R_H of StrHA composite might be one of the reasons for slipping down its glass transition temperature (T_g) value.

Differential Scanning Calorimetry

The DSC thermograms of pristine starch and StrHA40 are shown in Figure 5. The T_g is an important parameter in evaluating the performance of a polymer material. Although it is hard to detect for starch-based materials using DSC,[34,45] the T_g of starch-based materials has been determined precisely by DSC in this study and the results are depicted in Figure 5. It has been found that a small amount of change in E_H and R_H values has greater effect on T_g value, beside the effect of inherent properties of HA bioceramic. Here, the T_g of the pristine starch polymer film samples obtained at nearly 27.1 °C from DSC during heating, allows the amorphous chains to acquire less mobility.[5] Whereas the T_g of StrHA40 composite film sample was found at −1.9 °C, which is significantly lower than that of pristine starch.[46] It indicates that the amorphous chains might be free to acquire mobility due to the presence of moisture or adsorbed water molecules as shown

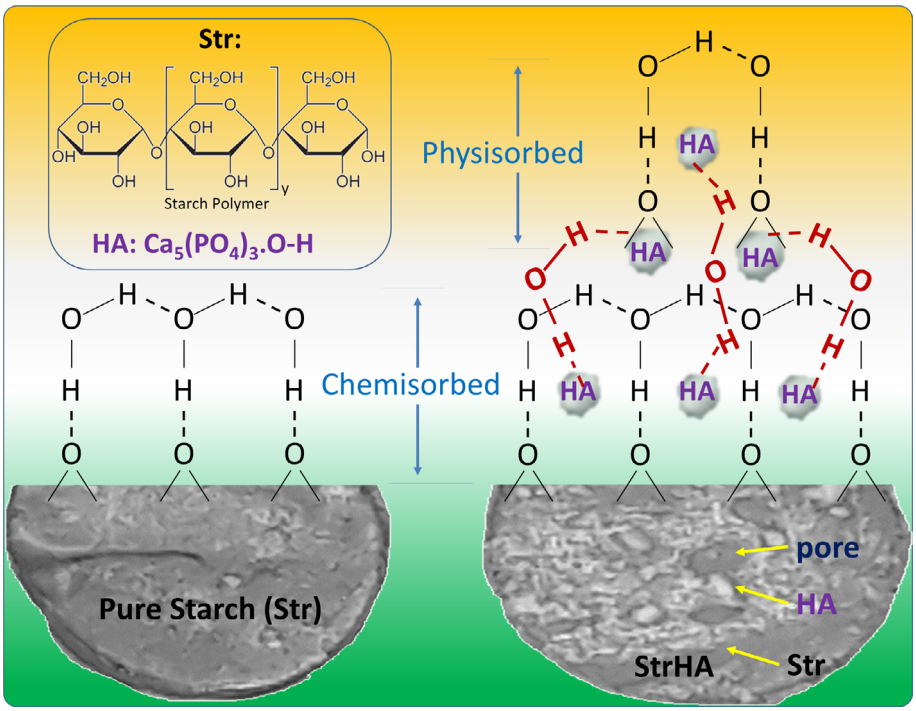

Figure 6. Schematic illustration of the hydrophilic mechanisms or water adsorption mechanisms of the pristine starch (Str) and Str–HA composite (right image); here, "…" is hydrogen bond and "—" is covalent bond. [Color figure can be viewed at wileyonlinelibrary.com]

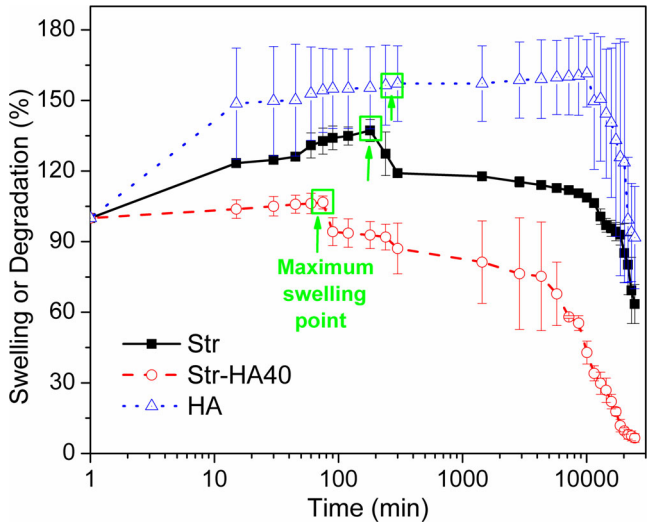

Figure 7. Swelling and degradation nature of pristine Str film, StrHA40 composite film, and pure HA scaffolds. [Color figure can be viewed at wileyonlinelibrary.com]

by endothermic peak at 99.99 °C. This could be because of addition of porous HA microparticle and/or nanoparticle in the composite. The less moisture content in pristine starch was obvious by showing of a small endothermic melting peak of starch at around 61.23 °C, which is very close to the result of pristine starch reported elsewhere.[47] It clearly indicates that the moisture content (i.e., used during synthesis) in the starch-based material also played a vital role in the structural, chemical as well as mechanical properties.

Mechanisms of Water Molecules Adsorption in Pristine Starch and StrHA Composite

From the FTIR as well as DSC studies, a schematic illustration of the hydrophilic mechanisms or water adsorption mechanisms of the pristine starch (Str) and Str–HA composite is depicted in Figure 6. Here, both the samples might have chemisorption but StrHA composite would have an additional layer of physisorption due to the porous HA nanoparticles.[48] The additional ability of hydrophilic adsorption through physisorption of the StrHA composite would significantly help to store more water molecules in order to further transfer it to the cells for some more time. Here, O—H particles of porous HA microparticle and/or nanoparticle played a significant role in the physisorption of water molecules by forming hydrogen bonds. Therefore, biodegradability of the starch-based plastics can also be tuned by using porous HA microparticle and/or nanoparticle.

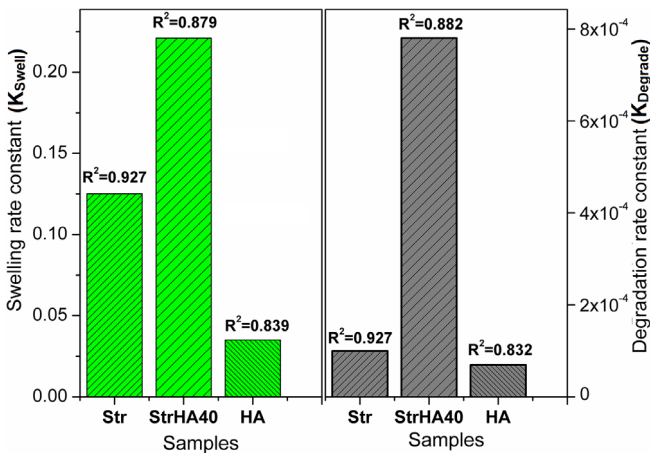

Figure 8. First-order swelling (K_{Swell}) and degradation ($K_{Degrade}$) rate constants of pristine Str film, StrHA40 composite film, and pure HA scaffolds. [Color figure can be viewed at wileyonlinelibrary.com]

In Vitro Swelling and Biodegradability

A comparison in *in vitro* swelling and biodegradability behaviors of the pristine starch (Str) film, composite (StrHA40) film, and pure HA thin film scaffolds is depicted in Figure 7. All the materials had shown first swelling in saline water while weight increased gradually, that is, hydrophilic in nature, and then degradation while weight decreased. Similar observation had also been noticed in other biopolymeric composites by other study.[33] It has been noticed that the saline water absorption saturated at different times for different materials, for example, 120 min for starch film, 75 min for StrHA40, and 300 min for HA; however, all the materials started to degrade after 3 days (4320 min). Further, more than 75 wt % of the StrHA40 composite still remained up to 3 days. Maximum degradation was found in the composite (StrHA40) compared to the pure HA and pristine starch. It occurred through two steps, first debonding of second phase HA particles from the starch matrix via physisorbed water molecules and then degradation of starch matrix, which acted as binder in the composites, via chemisorbed water molecules as illustrated in Figure 6. This result indicates that starch/HA-based composites can be used as a biodegradable scaffold which would need to degrade at least 3 days and maximum 15 days (where 15 wt % was remained) in tissue engineering applications, including skin implants.[17,49] This could be due to the result of steric hindrance effect of molecular —OH of HA on —CH_2—OH of starch. This steric hindrance helped to decelerate the unwanted side reactions. It could be more beneficial for external implants because after degradation, the HA particles would be rejected by scaffold gradually and thus, easy to remove from the skins.

Figure 8 represents the swelling and degradation kinetics in term of first-order rate constant values of the samples. In Figure 7, the green color arrows indicate the maximum swelling point of consideration. As per Figure 7 up to the maximum swelling point, the swelling rate constant (K_{Swell}) and after the maximum point up to the end of the test degradation rate constant ($K_{Degrade}$) were considered and also mentioned in Figure 8. This result revealed that both swelling (K_{Swell}) and degradation ($K_{Degrade}$) rate constants were highest for StrHA40 composite compared to pristine starch as well as pure HA. It happened for two main reasons. First, it is due to the more interconnecting pores formation at the polymer/ceramic (Str/HA) boundaries in the composites. Those interconnected pores played a crucial role in absorption (during swelling) and desorption (during degradation) of water.[33] Second, it could be owing to the steric hindrance of molecular —OH of HA on —CH_2—OH of starch to reduce the unwanted side reactions. Therefore, it evidently implies that the swelling and degradation rates of the starch or HA can be controlled by the making them into composites.

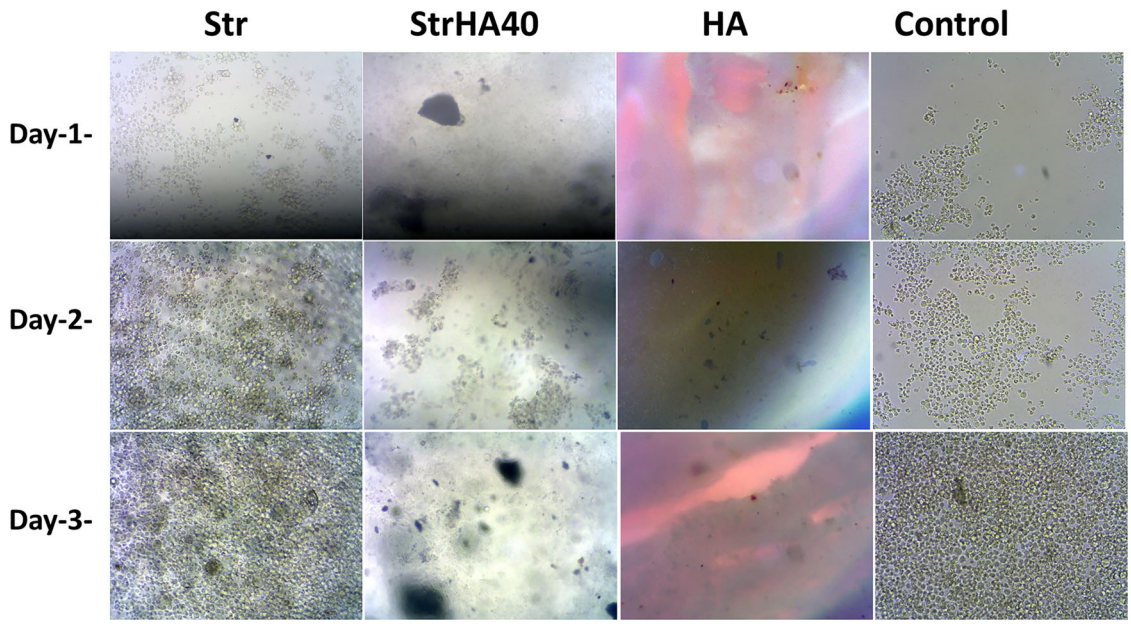

Figure 9. Optical micrographs of lymphocyte blood cell proliferation of pristine Str film, StrHA40 composite film, pure HA scaffolds, and a control (without any scaffold, only cells) after 1, 2, and 3 days on lymphocyte cells. [Color figure can be viewed at wileyonlinelibrary.com]

In Vitro Cell Culture Result

The optical micrographs were taken after Days 1, 2, and 3 to investigate the cell proliferation on to the surfaces of all the cultured samples. Figure 9 represents the optical micrographs of lymphocyte blood cell proliferation of starch film, composite (StrHA40) film, pure HA scaffolds and a control (without any scaffold, only cells) after 1, 2, and 3 days on lymphocyte cells. This result shows that the cell proliferation has increased with the cell culture time from Day 1 to Day 3. It can be noticed that the cells on pristine starch film were more visible compared to the other samples (StrHA40 composite film and pure HA). It is because of the fully transparent nature of pristine starch film compared to the other samples. The opacity was highest for pure HA. Interestingly, it was observed that the many cells grown homogeneously and distributed on the pristine starch surface whereas the cells were found to form flower-like colony on the surface of composite materials particularly at the HA particle-starch interfacial areas. This result evidently indicates that the HA particles enhanced the cell adherence properties of the starch. It was further confirmed by the MTT assay.

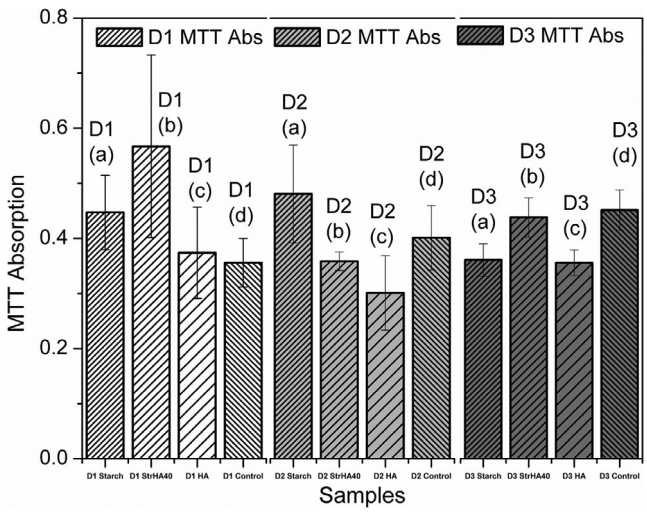

Figure 10. MTT absorption of pristine Str film, StrHA40 composite film, pure HA scaffolds, and a control (without any scaffold, only cells) after 1, 2, and 3 days on lymphocyte cells.

In the MTT assay (see Figure 10), the cell viability of pristine starch (Str) film, composite (StrHA40) film, pure HA scaffolds and a control (without any scaffold, only cells) after 1, 2, and 3 days on lymphocyte cells is depicted. The OD obtained was directly proportional to the number of viable cells.[33] This result depicts that the live cell viability has increased with the cell culture time from Day 1 to Day 3. However, the OD obtained in MTT assay on Day 3 was lesser than Day 1 due to a common phenomenon of overwhelming cell population, and also it was confirmed by the microscopic study in Figure 9 as similar as to the reported studies on other cells.[7,17,50] For the lymphocytes, it was found that after Day 1, the cells had grown very quickly and assembled a layer-like structure on top of the other cell layers on the scaffolds. This may cause cell death due to the overwhelming cell population and finally, reduce the OD of live cells on Day 3. It was also noticed that the OD of StrHA40 composite film was higher than that of pristine starch as well as pure HA. The additional ability of hydrophilic adsorption through porous micro- and/or nano-HA particles could be the main reason for improving cell quantity for long periods in MTT study. Therefore, our lymphocyte cells culture assay proved that the hematocytotoxicity of the starch/HA-based composite is very poor and thus, bioactivity of starch/HA composite to the blood cell would be excellent. Hence, this StrHA40 composite scaffold can be an excellent potential candidate for soft tissue or wound healing tissue engineering applications.

CONCLUSIONS

Starch polymer film has successfully been synthesized and fabricated from potato, which is a source of natural carbohydrate polymers, by a simple inexpensive one-pot synthesis technique. HA also has been produced from another natural source such as, goat bone. Therefore, starch/HA thin film composites-based biodegradable scaffolds synthesized by green technology would be cost-effective compared to the other synthetic biopolymer-based materials. The StrHA40 composite thin film had shown the best tensile strength (3.03 ± 0.03 MPa), elongation (21.5 ± 5.5%) as well as modulus (15.69 ± 0.17 MPa) which are very close to the human skin. In *in vitro* degradation study, it has been found that more than 76 wt % of the StrHA40 composite was still present up to 3 days. Controlled degradation found in the StrHA40 composite scaffolds was with two steps: first, debonding of second phase HA particles from the starch matrix and then, degradation of starch matrix. This result showed that the starch/HA composite-based biodegradable scaffolds can be used in those biomedical applications wherein the implants need to degrade between 3 and 15 days. The chemical structural characterizations had precisely been carried by FTIR and DSC study and it inferred a crucial information that the E_H and R_H values have a significant effect on T_g value. This study also postulated the probable adsorption mechanisms of water molecules by pristine starch as well as starch/HA composite films. The swelling as well as biodegradability of the StrHA40 composite film was very good compared to the pristine starch and pure HA. This study concluded that the biodegradability of the starch-based plastics can also be tuned by using porous HA microparticle and/or nanoparticle. Therefore, the variation in different biocompatibilities, degradation rates, and physical and chemical properties would be considered as effective strategies to develop starch-based completely biodegradable polymers for ideal biodegradable scaffolds in various applications. In StrHA composite film scaffold, physisorption of water molecules in addition to chemisorption played a crucial role to store extra water molecules in order to further transfer it to the cells for a longer period. For the first time, the lymphocytes compatibility of starch–HA composites study had been carried out in the present study. The StrHA40 scaffold had also shown excellent biocompatibility to the human blood cell derived lymphocytes. Therefore, the starch/HA composites thin film-based biodegradable scaffolds developed in the present study would be an excellent promising candidate for soft tissue regeneration and/or replacement applications.

ACKNOWLEDGMENTS

The authors acknowledge DSC Laboratory, Department of Mechanical Engineering and Nanotechnology Research Centre (NRC), SRM Institute of Science and Technology for accessing their research facilities such as DSC and XRD as well as FTIR, respectively.

CONFLICT OF INTEREST

The authors declare no potential conflict of interest.

REFERENCES

1. Jukola, H.; Nikkola, L.; Gomes, M. E.; Chiellini, F.; Tukiainen, M.; Kellomäki, M.; Chiellini, E.; Reis, R.; Ashammakhi, N. *J. Biomed. Mater. Res. B.* **2008**, *87*(1), 197.
2. Oliveira, A.; Pedro, A.; Arroyo, C. S.; Mano, J.; Rodriguez, G.; Roman, J. S.; Reis, R. *J. Biomed. Mater. Res. B: Appl. Biomater.* **2010**, *92*(1), 55.
3. Salgado, A.; Coutinho, O.; Reis, R.; Davies, J. *J. Biomed. Mater. Res. A*. **2007**, *80*(4), 983.
4. Liu, X.; Ma, P. X. *Annal. Biomed. Eng.* **2004**, *32*(3), 477.
5. Nogueira, G. F.; Fakhouri, F. M.; de Oliveira, R. A. *Carbohydr. Polym.* **2018**, *186*, 64.
6. Sartori, T.; Menegalli, F. C. *Food Hydrocoll.* **2016**, *55*, 210.
7. Latfi, A. S. A.; Pramanik, S.; Poon, C. T.; Gumel, A. M.; Lai, K. W.; Annuar, M. S. M.; Pingguan-Murphy, B. *J. Biomater. Appl.* **2019**, *33*(6), 854.
8. Gomes, M. E.; Reis, R. *Int. Mater. Rev.* **2004**, *49*(5), 274.
9. Liu, H.; Yu, L.; Simon, G.; Dean, K.; Chen, L. *Carbohydr. Polym.* **2009**, *77*(3), 662.
10. Guo, X.; Xiao, P.; Liu, J.; Shen, Z. *J. Am. Ceram. Soc.* **2005**, *88*(4), 1026.
11. Pramanik, S.; Kar, K. K. *Int. J. Adv. Manuf. Technol.* **2013**, *66*(5–8), 1181.
12. Deptuła, A.; Łada, W.; Olczak, T.; Borello, A.; Alvani, C.; Di Bartolomeo, A. *J. Non-Cryst. Solids*. **1992**, *147*, 537.
13. Pramanik, S.; Agarwal, A. K.; Rai, K.; Garg, A. *Ceram. Int.* **2007**, *33*(3), 419.
14. Fu, K.; Xu, Q.; Czernuszka, J.; Triffitt, J. T.; Xia, Z. *Biomed. Mater.* **2013**, *8*(6), 065007.
15. Razali, N. A. I. M.; Pramanik, S.; Abu Osman, N. A.; Radzi, Z.; Pingguan-Murphy, B. *J. Ceram. Process. Res.* **2016**, *17*(7), 699.
16. Ahmed, S.; Ahsan, M. *Bangladesh J. Sci. Ind. Res.* **2008**, *43*(4), 501.
17. Pramanik, S.; Ataollahi, F.; Pingguan-Murphy, B.; Oshkour, A. A.; Abu Osman, N. A. *Sci. Rep.* **2015**, *5*, 9806.
18. Ataollahi Oshkour, A.; Pramanik, S.; Shirazi, S. F. S.; Mehrali, M.; Yau, Y.-H.; Abu Osman, A. N. *Sci. World J.* **2014**, *2014*, 616804.
19. Boesel, L. F.; Mano, J. F.; Elvira, C.; San Roman, J.; Reis, R. L. Biodegradable Polymers and Plastics; Springer: Boston, MA, **2003**; p 243.
20. Boesel, L. F.; Mano, J. F.; Reis, R. L. *J. Mater. Sci.-Mater. Med.* **2004**, *15*(1), 73.
21. Nofrarías, M.; Martínez-Puig, D.; Pujols, J.; Majó, N.; Pérez, J. F. *Nutrition*. **2007**, *23*(11–12), 861.
22. Morrison, C.; Macnair, R.; MacDonald, C.; Wykman, A.; Goldie, I.; Grant, M. *Biomaterials*. **1995**, *16*(13), 987.
23. Ciapetti, G.; Granchi, D.; Verri, E.; Savarino, L.; Cavedagna, D.; Pizzoferrato, A. *Biomaterials*. **1996**, *17*(13), 1259.
24. Mendes, S. C.; Reis, R.; Bovell, Y. P.; Cunha, A.; van Blitterswijk, C. A.; de Bruijn, J. D. *Biomaterials*. **2001**, *22*(14), 2057.
25. Jane, J. *J. Macromol. Sci. Part A*. **1995**, *32*(4), 751.
26. Pramanik, S.; Pingguan-Murphy, B.; Cho, J.; Abu Osman, N. A. *Sci. Rep.* **2014**, *4*, 5843.

27. Marques, A.; Reis, R.; Hunt, J. *Biomaterials*. **2002**, *23*(6), 1471.
28. Moradi, A.; Pramanik, S.; Ataollahi, F.; Kamarul, T.; Pingguan-Murphy, B. *Anal. Methods*. **2014**, *6*(12), 4396.
29. Puppi, D.; Piras, A. M.; Detta, N.; Ylikauppila, H.; Nikkola, L.; Ashammakhi, N.; Chiellini, F.; Chiellini, E. *J. Bioact. Compat. Polym.* **2011**, *26*(1), 20.
30. Puri, B.; Sharma, L.; Pathania, M. Principles of Physical Chemistry. Chapter 28; Vishal Publishing: Jalandhar, **2012**. p. 1033.
31. Sarkar, K.; Han, S.-S.; Wen, K.-K.; Ochs, H. D.; Dupré, L.; Seidman, M. M.; Vyas, Y. M. *J. Allergy Clin. Immunol.* **2018**, *142*(1), 219.
32. Sarkar, K.; Bose, A.; Chakraborty, K.; Haque, E.; Ghosh, D.; Goswami, S.; Chakraborty, T.; Laskar, S.; Baral, R. *Vaccine*. **2008**, *26*(34), 4352.
33. Diba, M.; Kharaziha, M.; Fathi, M.; Gholipourmalekabadi, M.; Samadikuchaksaraei, A. *Compos. Sci. Technol.* **2012**, *72* (6), 716.
34. Li, M.; Liu, P.; Zou, W.; Yu, L.; Xie, F.; Pu, H.; Liu, H.; Chen, L. *J. Food Eng.* **2011**, *106*(1), 95.
35. Kar, K. K.; Pramanik, S. U.S. Pat. 8,652,373 B2 (**2014**).
36. Stasiak, M.; Molenda, M.; Opaliński, I.; Błaszczak, W. *Czech J. Food Sci.* **2013**, *31*(4), 1212.
37. Combrzynski, M.; Moscicki, L.; Rejak, A.; Wójtowicz, A.; Oniszczuk, T. *Teka Komisji Motoryzacji i Energetyki Rolnictwa*. **2013**, *13*, 2.
38. Ankersen, J.; Birkbeck, A. E.; Thomson, R. D.; Vanezis, P. *Proc. Inst. Mech. Eng. H.* **1999**, *213*(6), 493.
39. Hebeish, A.; Aly, A.; El-Shafei, A.; Zaghloul, S. *Egypt. J. Chem.* **2009**, *52*, 73.
40. Rachtanapun, P. Carboxymethyl cellulose from papaya peel/corn starch film blends. In Kasetsart University Annual Conference, Bangkok (Thailand), 17–20 March **2009**.
41. Qin, C.; Huang, K.; Xu, H. *Carbohydr. Polym.* **2002**, *49*(3), 367.
42. He, F.; Yang, Y.; Yang, G.; Yu, L. *Z. Naturforsch.* **2008**, *63* (3–4), 181.
43. Haniffa, M. A. C. M.; Ching, Y. C.; Chuah, C. H.; Ching, K. Y.; Nazri, N.; Abdullah, L. C.; Nai-Shang, L. *Carbohydr. Polym.* **2017**, *173*, 91.
44. Poletto, M.; Ornaghi, H.; Zattera, A. *Materials*. **2014**, *7*(9), 6105.
45. Liu, P.; Yu, L.; Liu, H.; Chen, L.; Li, L. *Carbohydr. Polym.* **2009**, *77*(2), 250.
46. Averous, L.; Fauconnier, N.; Moro, L.; Fringant, C. *J. Appl. Polym. Sci.* **2000**, *76*(7), 1117.
47. Yu, L.; Christie, G. *Carbohydr. Polym.* **2001**, *46*(2), 179.
48. Tripathy, A.; Sharma, P.; Sahoo, N.; Pramanik, S.; Abu Osman, N. A. *Sens. Actuat. B-Chem.* **2018**, *262*, 211.
49. Moradi, A.; Ataollahi, F.; Sayar, K.; Pramanik, S.; Chong, P. P.; Khalil, A. A.; Kamarul, T.; Pingguan-Murphy, B. *J. Biomed. Mater. Res. Part A*. **2016**, *104*(1), 245.
50. Pramanik, S.; Kar, K. K. *J. Appl. Polym. Sci.* **2012**, *123*(2), 1100.